International Journal of Computing and Artificial Intelligence

E-ISSN: 2707-658X
P-ISSN: 2707-6571
www.computersciencejournals.com/ijcai
IJCAI 2024; 5(1): 30-37
Received: 02-12-2023
Accepted: 06-01-2024

Ahmed Fraidoon Abdulkarem
Department of Computer Engineering, Information Technology, Altinbas University, Istanbul, Turkey

Corresponding Author:
Ahmed Fraidoon Abdulkarem
Department of Computer Engineering, Information Technology, Altinbas University, Istanbul, Turkey

Image quality enhancement and rain removal on images taken under different rain conditions

Ahmed Fraidoon Abdulkarem

DOI: https://doi.org/10.33545/27076571.2024.v5.i1a.80

Abstract
The Deep Detail Network (DDN) was created to eliminate rain streaks from photographs. Deep convolutional neural networks (CNN) are taught with data to learn how to correlate rainy and clean feature layers in pictures. We create our own rainy photos for training because we do not have access to real-world ones. BCET enhances contrast in low-light pictures by modifying the objective function and adjusting contrast, rather than simply increasing the network's depth or breadth. We trained our Deep Neural Network (DDN) using two datasets of rainy photos. Testing DDN on actual images revealed that the network achieved good performance, even though it was trained on artificial data. Image processing is utilized to enhance the visual outputs of the CNN architecture. Improvements in rain removal include enhancing the contrast in wet and low-light photographs and increasing the computational speed after implementing a new network, surpassing previous approaches.

Keywords: Deep learning, contrast enhancement, rain removal, deep detail network

1. Introduction

Rain, a prevalent kind of adverse weather, can reduce image sharpness and damage outdoor visual equipment. Rain streaks can cause a hazy look in pictures due to light dispersion. Many practical applications require effective methods for removing rain streaks. These features encompass photo enhancement, object detection, and tracking. Adverse weather conditions might negatively impact image processing procedures. The algorithms provide outputs based on feature data extracted from photos captured by various sources. Therefore, it is crucial to develop algorithms that are resilient to weather fluctuations. There are now two types of rain removal techniques: one for films and one for still photographs. Images captured in rainy conditions include unnecessary temporal data, making it simpler to identify and eliminate rain streaks. The researcher in [1] proposed A rain streak based on correlation recognition algorithm. The method identifies the location of rain streaks and eliminates them by calculating the average pixel values from neighboring frames. Barnum *et al*. have created a frequency-space representation of the visual impact of rain. A streak direction distribution is utilized to predict rainfall in reference [3]. Phase consistency is utilized in [4] to identify and remove rain streaks by minimizing registration errors between frames. Several strategies are useful, but the temporal aspect of video enhances their effectiveness significantly. We focus on removing rain in this project from a single picture.

The authors suggested segmenting dynamic situations using a motion segmentation-based method. They used photometric and color constraints to identify rain, then used dynamic features and motion interference cues to apply rain removal masks on pixels. Rain pixels were recovered by utilizing both spatial and temporal information. The hybrid feature set [6] was used to decrease the presence of rain while enhancing non-rain elements. An investigation was conducted on picture deconstruction and self-learning methods for improving image quality and removing rain. The approach described in reference [7] begins by doing context-constrained picture identification. Various types of dictionaries will interchange atoms that correspond to rain patterns. The approach described in reference [7] uses classifiers on collected language sets to automatically identify frequent rain patterns and eliminate rain as a high-frequency component. The methods mentioned by MCA, Fu, Yu-Hsiang, *et al*. [8] are insufficient and need advanced expertise. A camera's primary purpose is to capture images, but the idea of photography has evolved since the period of black and white cameras. The objective is to remove the object's shadows and then take a 2D picture.

Spatial domain coordinates define a two-dimensional image [9]. A digital image consists of a finite set of visual components, often known as pixels, each of which has a unique amplitude and position. An image's digital components are represented by each pixel. There are several uses for digital image processing [10]. The number of pixels that are present in a digital image is called picture resolution. Whatever the lens setting, sharper and higher-quality photos are produced with smaller pixels. There may be more pixels in images with smaller pixel sizes. The data of the image is represented by the number of pixels. The pixel resolution is 7680 x 6876, where the first number indicates the picture width (columns) and the second number indicates the image height (rows). Pixel specifications broken down by size or region, such pixels per inch, are part of additional standards. 2,097,152 pixels make up a picture of 1024 x 2048 pixels.

Enhancing picture quality, improving core vision algorithms, and adding multi-modal sensors to the sensor module are three techniques to address wet weather in automated image surveillance. This endeavor will focus on analyzing raw picture data to reduce and study the dynamic impacts of rain and snowfall through augmentation and analysis. Their methodologies are believed to enhance traditional vision techniques such as fragmentation, identification, and monitoring, making them more effective. We will conduct a quantitative analysis of this claim in order to offer new insights to the scholarly community. Currently, the authors' recordings or still photos are used to assess rain removal techniques. To create synthetic datasets, rain streaks are placed on photos without any rain [11]. Rain removal algorithms are frequently trained and tested using indoor images captured with fake rain.

Rain can reduce picture quality and have a detrimental impact on outdoor machine vision. Rain streaks generate haziness in photographs due to light dispersion when it rains. Improved rain removal techniques are needed for several practical applications, including contrast enhancement and motion detection. We have concentrated on techniques for rain removal and picture analysis that include modifying camera settings, along with other methodologies. Changing the camera settings on a camcorder does not allow the user to access previously captured photographs or movies. However, existing component-based strategies for eliminating raindrops from video may provide distorted results.

Moreover, for instance, rain might have anticipated effects, such rain running along many advancing edges that could harm the pixel. Tasks like visual requests, object identification, image selection, astonishment, and picture stitching rely significantly on extracting rotational and scale-invariant point-based features from pictures.

This project will use machine-learning methods to identify rain drops. Moreover, Both directed and bilateral filters are used in noise reduction. The rain-affected photographs were improved using machine learning and a histogram for image comparison. The Python programming language will be used to create the graphical user interface. Digital photographs will be employed to enhance and assess image resolution using an innovative approach in the architecture.

2. Methodology

The section on methodology offers details on the algorithmic assistance and computational strategy utilized to extract data from interacting information processes for processing and analyzing visual data in image processing and analysis under different temperature scenarios. Figure 1 presents an illustration of the suggested system.

If it is impossible to acquire data that directly depicts the poor quality of the rain. Machine learning was utilized to solve the problem, and the algorithmic software that was created improved the accuracy of photographs captured under rainy conditions, as well as facilitated feature extraction and analysis. The chapter explains a deep neural network learning approach and its use in improving photographs taken in unfavorable weather conditions. Improving image quality will raise object identification accuracy in wet conditions, which is crucial for security cameras and object prediction.

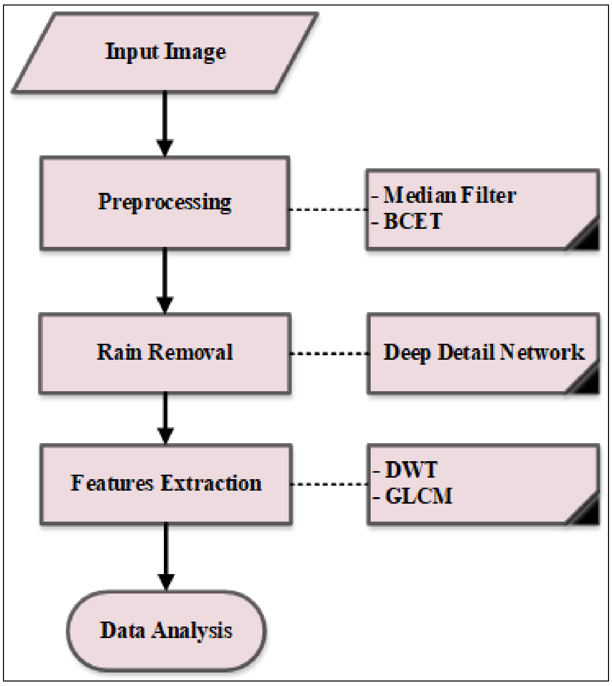

Fig 1: The flowchart of recommended system

2.1 Improving the contrast of images

The primary purpose of preprocessing is to enhance the image quality of the specific local region captured by several cameras in wet conditions. A shape is formed that is appropriate for further processing by machine vision systems or humans. Moreover, pretreatment enhances key picture properties, as listed below [14]:

Pre-major processing is utilized to improve the picture characteristics captured in damp environments. Eliminates background noise, enhances picture quality, and improves several metrics in this phase. For noise reduction, an early phase involved using a median filter with varying picture set performance. Weights were calculated according on the distance between successive rainy images. It functions as a preliminary stage in creating the frequency distribution-based filter known as the median [15]. An adaptive weight adjustment technique based on neighboring photos improves the noise reduction quality. Figure 2 illustrates the histogram building method that considers weight.

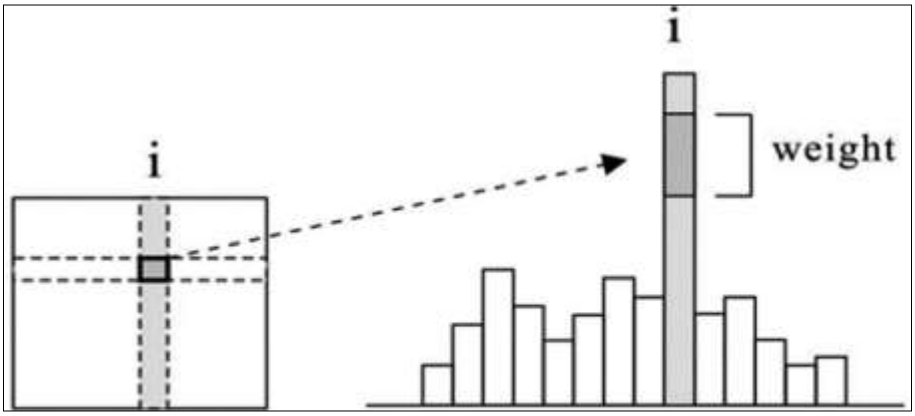

Fig 2: Scheme of weighted median filter histogram formation

Ability to calculate textural features and examine the structural characteristics of the lesion using brightness representation in the rainy image. We then utilize adaptive contrast enhancement using the modified algorithm given in reference [17] to improve the signal-to-noise ratio. Thus, enhancing the clarity of the first MRI scans. The primary challenge is in the inadequate picture quality for efficient extraction, analysis, recognition, and quantitative measurement of parameters. Medical pictures sometimes contain impulsive, multiplicative, or additive noise due to imperfections in the imaging process. The writers in references [18] and [19] suggested utilizing Contrast Balance Enhancement Technique (CBET) technology to enhance the contrast of the region of interest. The region of interest in medical imaging need contrast.

The findings indicate that the mean values of all channels have been equalized following the use of the BCET solution. Figure 3 displays one example.

Fig 3: Example of color image processing with BCET

2.2 Image de-raining

Rain streaks in video and image processing can cause a notable decrease in performance. Recently, several researchers in the field of computer vision and image processing have been concentrating on developing methods to remove rain from videos and photos.

To improve object recognition results, we aim to eliminate rain noise streaks from individual photos. Develop a real-time-efficient system capable of functioning in adverse weather circumstances, such as rainy days, to assist visually impaired individuals in their regular activities.

An in-depth architecture for rain removal was explored following the significant achievements of deep neural networks. This system utilizes a deep convolutional neural network (CNN). The Res-Net is crucial for the network's functionality [20, 21]. Res-Net intends to alter the mapping form to streamline the learning process. Deep convolutional neural networks were employed to remove rain streaks from a single image, demonstrating the same principle.

We required a rain removal approach that maintains image quality as the result would be utilized in object recognition. We examined an algorithm known as Deep Detail Network (DDN), which has the greatest qualitative and quantitative metrics for this purpose. The algorithm's general framework is depicted in Figure 4.

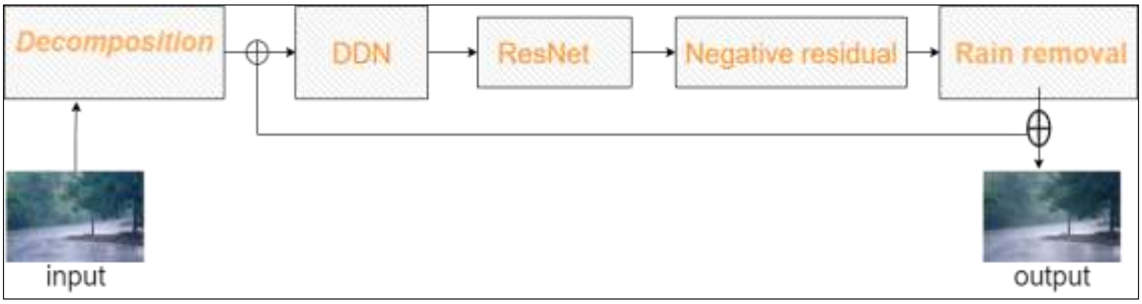

Fig 4: Structure of the framework for rain removal algorithm from the image

2.2.1 General idea (negative residual mapping and deep detail structure)

The suggested study utilizes rain streak characteristics to improve the network outcome and introduce a form of bias. The authors initially used a normal deep convolutional neural network, however the results were unsatisfactory, as seen in Figure 5.

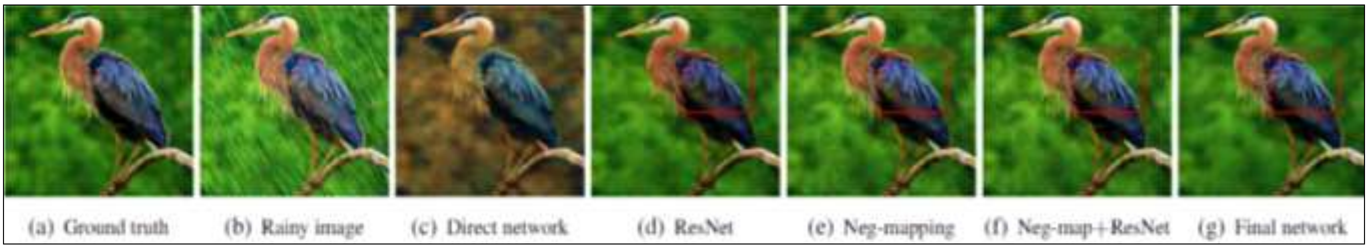

Fig 5: De-rained results of different network structures [4]

In Figure 5.c, the direct network altered the image color space, eliminating rain and modifying the pixel range in the image. The researcher simplifies the explanation by normalizing photographs X and Y to a range of [0-1] with D pixels. The regression function mapping from $[0, 1]^D$ to $[0, 1]^D$ for these pictures must be determined. This involves assigning a range that encompasses all pixel values to the regression algorithm. Training a deep neural network (DDN) on photos might encounter issues with vanishing gradients, even when regularization approaches like batch normalization are applied (Figure 6).

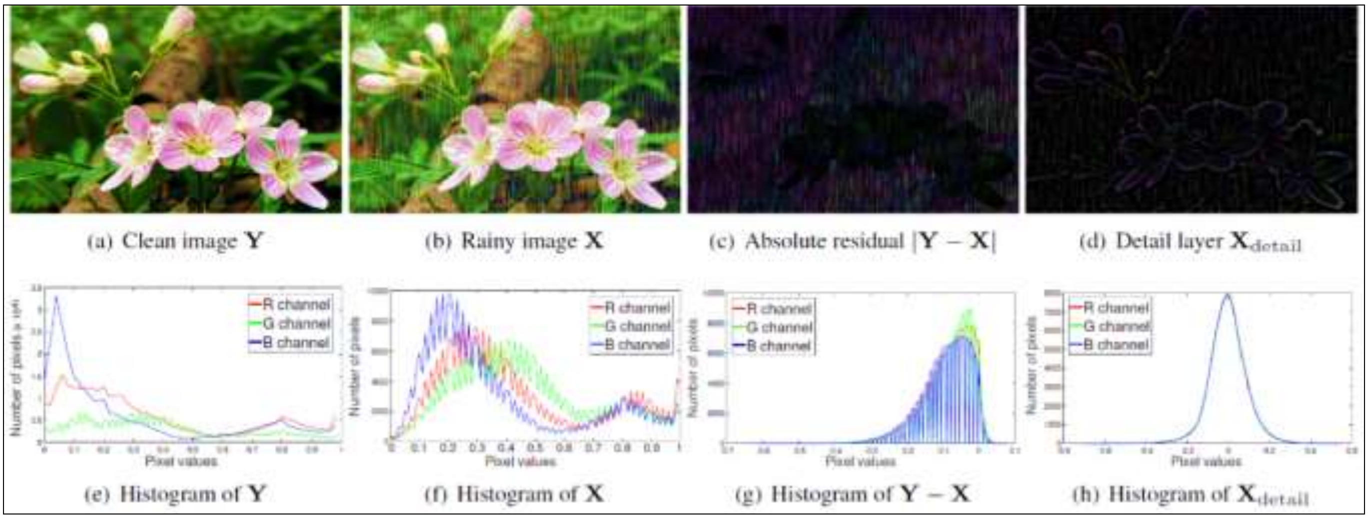

Fig 6: Range reduction, detail layer, and negative residual sparsity. |Y-X| to improve the visualization [20]

Enhancing network knowledge is crucial for reducing the space required for mapping operations. Figure 6 (e) and (g) depict the clean picture Y and the difference between the blurry picture Y - X, which shows a significant reduction in pixel units. The residue can be incorporated into the network to help establish the mapping. They used the leftover as a result of the parameter layers depicted in Figure 3.

This direct skip connection may produce lossless data over the whole network, which is useful for assessing the final de-rained image. The contrast between Y and X may be negative in most circumstances due to the appearance of rain as white streaks in images (Figure 6 (g)). Referred known as negative residual mapping, abbreviated as neg-mapping. A refined goal that combines the idea:

$$\mathcal{L} = ||h(Xi\ ) + Xi - \ Yi\ ||_F^2 \qquad (1)$$

Figure 6 (d) demonstrates how the Res-Net model's de-raining procedure was modified to overcome the constraints of image regression. The original Res-Net structure does away with rain streaks, which makes the bird's feathers appear blurry. The details of the color and object are shown in Figure 6(e) using neg-mapping instead of the Res-Net structure. This happens as a result of the lossless data being updated and spread straight across parameters via skip links. Compared to Res-Net, Neg-mapping needs less training and has fewer testing errors.

Over time, some rain streaks were still visible in the images that were taken. This suggests that the broadcast does not fully acknowledge rain streaks and protest places of interest. This leads to the subsequent advancements of the negative mapping concept.

Implementing a Res-Net structure with neg-mapping can enhance the capacity and flexibility to analyze and represent picture information, namely distinguishing Rain trails from details on other objects. The input information in this structure is ensured and propagates across all parameter levels to train the network. Figure 6 (f) demonstrates that there are still some little rain streaks visible in the resulting image despite using both methods together. The Res-Net technique differs from the input of from the parameter layers to the detail layer. The initial model is as follows:

$$X = X_{detail} + X_{base} \quad (2)$$

The foundation layer is commonly known as a 'detail' and 'specifics'. After acquiring the base layer by X [22-24] reduced filtering, the feature layer implemented X detail = X-X base. After removing the foundation layer from the image, only rain patterns and object shapes remain in the detail layer, as seen in Figures 6 (d) and (h). The sparsity of the detail layer is greater than that of the picture since most areas are close to zero. The present de-rain approaches do not utilize this sparsity, unlike the pure framework of deep learning.

Besides, Figures 6 (c), (d), (g), and (h)show "Detailed layers and leftover rejection both display critical extend lessening". Hence, the viable mapping is produced by littler subsets of $[0, 1]^D$ to $[0, 1]^D$ [80]. Showing the network space contracted and thus network execution ought to be progressed.

The input to the Res-Net parameter layers facilitates the integration of the detail layer Xdetail with the recommended neg-mapping Y − X. Scholars refer to the network trained on the detail layer as the "deep detail network." The final output in Figure 5(g) outcomes of combining neg-mapping and the deep detail network. Together with a stronger structural similarity index (SSIM) and a higher convergence rate, this outcome also produces a more pronounced visual de-raining effect.

3. Result and Discussions

Both throughout this investigation and via the https://www.imaging-resource.com/IMCOMP/COMPS01.HTM, image datasets were gathered. A dataset made up of pictures taken with different cameras, including pictures taken during wet weather and YTVOS201 pictures taken during clear weather as well as pictures or videos taken during regular circumstances. By employing an algorithm to eliminate rain and assessing the outcomes using PSNR and SSIM metrics, the objective is to improve object detection. To confirm the correctness of the technique, the object detection algorithm (YOLOV3) is also evaluated on the photos both before and after processing.

3.1 Contrast enhancement

Here are some examples of results (low light image contrast enhancement with histogram) shown in Figures 7, from left to right, the first column indicates the input image and the second column represents the output images.

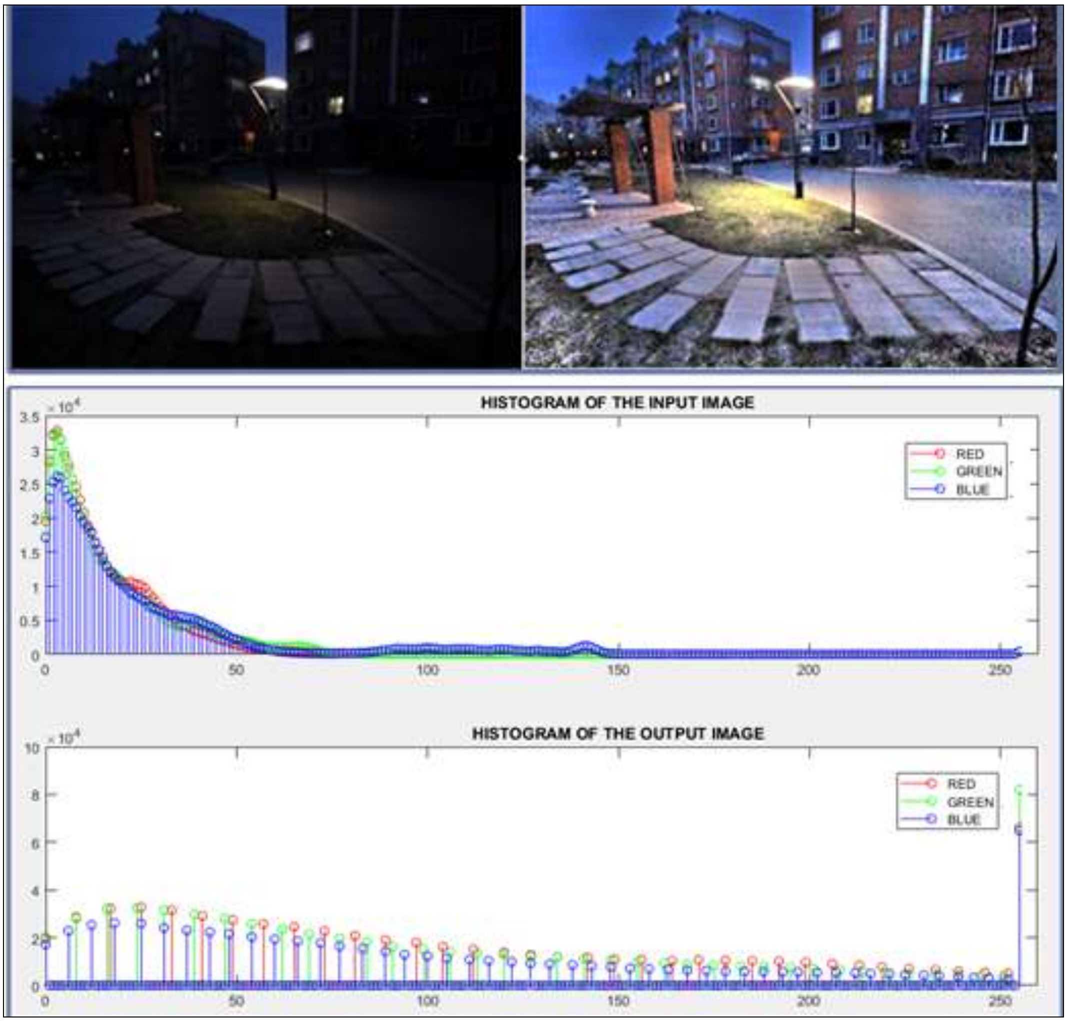

Fig 7: Low contrast image enhancement 1

3.2 De-raining results

To assess the results of the updated method of de-raining images and real films, two datasets were employed. For the YTVOS201 dataset, the experimental results are displayed in Figure 8, and the dataset results are displayed in Figure 9.

Fig 8: Results of the de-raining algorithm on the YTVOS201 dataset

Fig 9: Results of the de-raining algorithm on a Rainy image dataset

Table 1 demonstrates quantitative results of all competing methods on synthetic images from Figures 3 and 4. From the table, we can conclude that the proposed algorithm for rain removal is more effective.

Table 1: Evaluation of the performance of PSNR and SSIM on four synthetic images

Images	PSNR	SSIM	Rain Removed %
Image 1	15.47	0.898	94%
Image 2	17.33	0.915	95%
Image 3	15.96	0.923	96%
Image 4	18.51	0.982	97%
Image 5	13.91	0.945	95%
Image 6	14.62	0.952	98%

The comparative findings with alternative rain removal technologies are shown in Table 2.

The method successfully removes rain streaks from the rainy picture dataset but is less effective in removing rain streaks from the YTVOS201 dataset. The rain streaks in the YTVOS201 dataset photographs are larger and unrealistic, which results in the presence of rain, shadows, or markings in the images. Based on Figure 4.5, our results provide higher clarity compared to other approaches, with an error rate lower than other methods being tested. The PSNR is 31.374 and SSIM is 0.9437. Other approaches result in gathering some rain and compromising the image quality and contrast.

Table 2: Comparisons with other methods using PSNR and SSIM on the test Rainy image

Approach	PSNR	SSIM
DCPDN [29]	18.588	0.8329
DAF-Net [30]	21.063	0.8713
DID-MDN [31]	18.863	0.8331
RESCAN [32]	18.238	0.8288
Our Method	31.374	0.9437

3.2.1 De-raining with object detection results

We utilized two distinct picture datasets including objects of varying sizes and locations. The first dataset, Rainy image, consists of 100 photos with 120 items, while the second dataset, YTVOS201, has 25 images with 37 objects. After individually assessing each segment (object detection before and after de-raining). Table 3 displays the true positives, true negatives, false positives, and false negatives generated by the models on the test dataset.

Table 3: The Calculated Values of the Algorithms before and after De-raining

Dataset	No of Objects	Before processing			After processing		
		True Positives	False Positives	False Negatives	True Positives	False Positives	False Negatives
Rainy Images Dataset	120	90	11	15	**105**	**8**	**3**
YTVOS201 Dataset	37	20	10	3	**27**	**4**	**2**

The Precision, Recall, and F1 scores for each dataset are derived from the numbers in Table 3. Our methodology's average item detection findings are more accurate after processing compared to other approaches, including those before processing. Hence, the outcomes post-processing are more precise in object detection compared to pre-processing. The Precision, Recall, and F1 scores for each dataset are displayed in Figure 10.

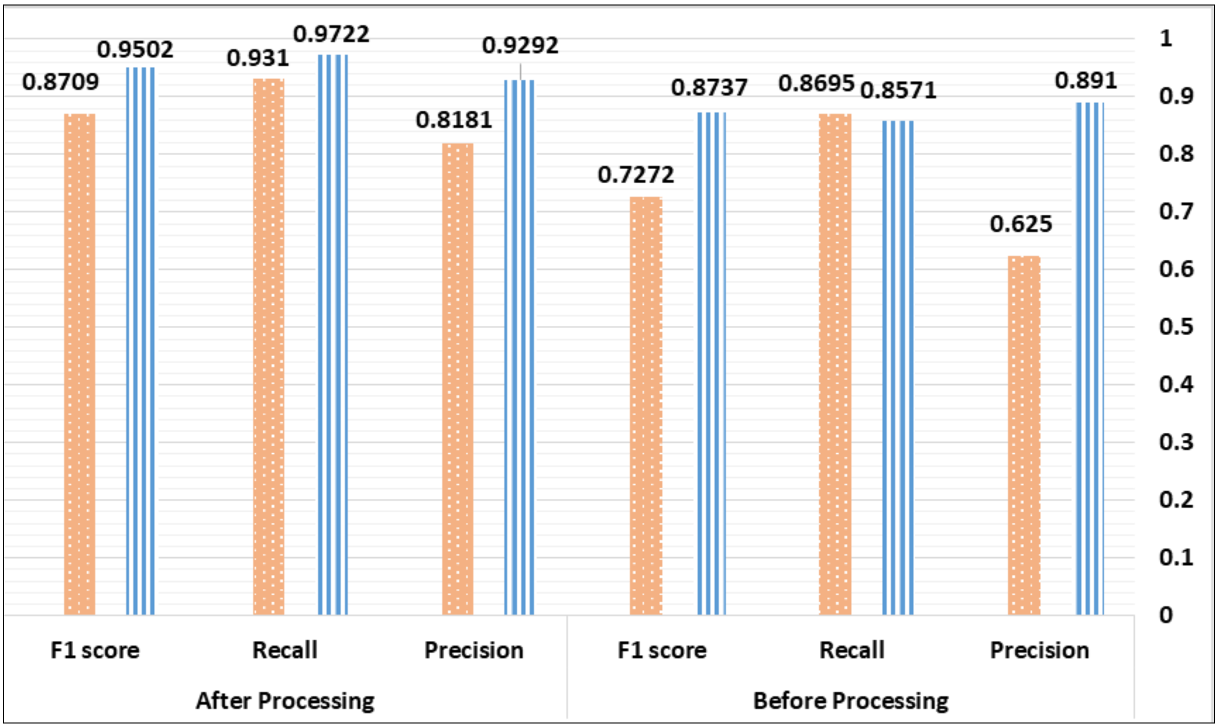

Fig 10: Evaluating the performance both before to and during image processing, of object detection

Figure 10 shows improved item detection after processing, with findings from our technology being more accurate than others, demonstrating its usefulness.

There are three different levels of object recognition in computer media, which improves the effectiveness of rain removal and contrast enhancement for detecting small items or objects partially visible in a frame, like a raindrop. Due to the site being scaled, objects on the opposite side may appear smaller in some instances.

The studies show that the suggested solution successfully restores the original image's identification accuracy. The method enhances average item detection under various levels of rain intensity. The results further highlight the significance of the de-raining module. Prior methods failed to accurately identify pedestrians even after evaluating pedestrian datasets during wet events. During wet days, our method accurately detects pedestrians.

The accuracy of the models for detecting objects was 87.06% for YOLOv3 before using the de-raining method and increased to 96.55% after its implementation. On the YTVOS201 Dataset, the accuracy was 90.90% for YOLOv3 before image processing and improved to 93.96% after using the De-raining method with YOLOv3.

Conclusion

A deep learning architecture called DDN with BCET was utilized to enhance contrast in wet images and eliminate rain. The approach employs a deep neural network to understand the conversion matrix from clean to moist picture detail layers. We generate pairings of clean and rainy photos to train a network, despite the absence of actual clean photographs corresponding to genuine rainy images. We demonstrate that this network effectively translates to real-world images. Convolutional neural networks are commonly utilized for complex visual tasks, but we demonstrated their effectiveness in processing real-world pictures in difficult situations. DDN with BCET outperforms other current methods in terms of image quality and processing speed.

References

1. Yang W, Tan RT, Feng J, Guo Z, Yan S, Liu J. Joint rain detection and removal from a single image with contextualized deep networks. IEEE Trans Pattern Anal Mach Intell. 2019 Jun;42(6):1377-93.
2. Park K, Kim M, Lim H, Yu S, Paik J. Fast Rain Removal Using Rain Map and Temporal Filtering for Consumer Imaging Applications. In: 2018 IEEE 8th International Conference on Consumer Electronics-Berlin (ICCE-Berlin). IEEE; c2018 Sep. p. 1-2.
3. Bahnsen CH, Moeslund TB. Rain removal in traffic surveillance: Does it matter. IEEE Trans. Intell. Transp. Syst. 2018 Aug;20(8):2802-19.
4. Xu J, *et al*. Removing rain and snow in a single image using the guided filter. In: Computer Science and Automation Engineering (CSAE), 2012 IEEE International Conference on. IEEE, 2012, 2.
5. Chen J, Chau LP. A rain pixel recovery algorithm for videos with highly dynamic scenes. IEEE Trans. Image Process. 2014 Mar;23(3):1097-1104.
6. Chen DY, Chen CC, Kang LW. Visual depth guided color image rain streaks removal using sparse coding. IEEE Trans Circuits Syst. Video Technol. 2014 Aug;24(8):1430-1455.
7. Yang W, Tan RT, Feng J, Liu J, Guo Z, Yan S. Deep joint rain detection and removal from a single image. In: Proceedings of the IEEE conference on computer vision and pattern recognition; c2017. p. 1357-1366.
8. Wang H, Xie Q, Zhao Q, Meng D. A model-driven deep neural network for single image rain removal. In: Proceedings of the IEEE/CVF Conference on Computer Vision and Pattern Recognition; c2020. p. 3103-3112.
9. Selami AM. Analysis of Image Features Taken from Different Camera Types. Muthanna J Eng. Technol. (MJET), 2018, 6(2).

10. Godínez-Rodríguez E, Ortíz MP, Balankin A, Carapia RF, Ortíz JP, García VMS, *et al*. Encriptado de Imágenes Basado en Advanced Encryption Standard y Caos. Rev Cubana Ing. 2021;12(2):e278-e278.
11. Yang W, Tan RT, Feng J, Liu J, Guo Z, Yan S. Deep joint rain detection and removal from a single image. In: Proceedings of the IEEE Conf. Comput. Vis. Pattern Recognit; c2017 Jul. p. 1-10.
12. Sara U, Akter M, Uddin MS. Image quality assessment through FSIM, SSIM, MSE, and PSNR: A comparative study. J Comput. Commun. 2019;7(3):8-18.
13. Liu YF, Jaw DW, Huang SC, Hwang JN. Desnow Net: Context-aware deep network for snow removal. IEEE Trans Image Process. 2018 Jun;27(6):3064-3073.
14. Justusson BI. Median filtering: statistical properties. In: Two-Dimensional Digital Signal Processing II. Springer, Berlin, Heidelberg; c1981. p. 161-196.
15. Loupas T, McDicken WN, Allan PL. An adaptive weighted median filter for speckle suppression in medical ultrasonic images. IEEE Trans Circuits Syst. 1989 Jan;36(1):129-135.
16. Zotin A. Fast algorithm of image enhancement based on multi-scale Retinex. Procedia Comput. Sci. 2018;131:6-14.
17. Tang C, Von Lukas UF, Vahl M, Wang S, Wang Y, Tan M. Efficient underwater image and video enhancement based on Retinex. Signal Image Video Process. 2019;13(5):1011-1018.
18. Dietrich CF, Averkiou M, Nielsen MB, Barr RG, Burns PN, Calliada F, *et al*. How to perform contrast-enhanced ultrasound (CEUS). Ultrasound Int. Open. 2018;4(01):E2-E15.
19. Ma J, Fan X, Yang SX, Zhang X, Zhu X. Contrast limited adaptive histogram equalization-based fusion in YIQ and HSI color spaces for underwater image enhancement. Int. J Pattern Recognit. Artif. Intell. 2018;32(07):1854018.
20. Fu X, Huang J, Zeng D, Huang Y, Ding X, Paisley J. Removing rain from single images via a deep detail network. In: IEEE Conf. Comput. Vis. Pattern Recognit; c2017. p. 1063-6919.
21. He KM, Zhang XY, Ren SQ, Sun J. Deep residual learning for image recognition. In: Proceedings of the IEEE Conf. Comput. Vis. Pattern Recognit. (CVPR); c2016. p. 770–778.
22. He K, Sun J, Tang X. Guided image filtering. IEEE Trans Pattern Anal. Mach Intell. 2013 Jun;35(6):1397-1409.
23. Tomasi C, Manduchi R. Bilateral filtering for gray and color images. In ICCV; c1998.
24. Zhang Q, Shen X, Xu L, Jia J. Rolling guidance filter. In: ECCV; c2014.
25. Huang DA, Kang LW, Wang YCF, Lin CW. Self-learning-based image decomposition with applications to single image denoising. IEEE Trans Multimedia. 2014 Jan;16(1):83-93.
26. Kang LW, Lin CW, Fu YH. Automatic single image-based rain streaks removal via image decomposition. IEEE Trans Image Process. 2012 Apr;21(4):1742-1755.
27. Fu X, Huang J, Zeng D, Huang Y, Ding X, Paisley J. Removing rain from single images via a deep detail network. In: IEEE Conf. Comput. Vis. Pattern Recognit. c2017. p. 1063-6919.
28. Minghan Li, Xiangyong Cao, Qian Zhao, Lei Zhang, Deyu Meng. Online rain/snow removal from surveillance videos. IEEE Trans Image Process. 2021.
29. Zhang H, Patel VM. Densely connected pyramid dehazing network. In: Proceedings of the IEEE Conf Comput Vis Pattern Recognit. 2018. pp. 3194-3203.
30. Hu X, Fu CW, Zhu L, Heng PA. Depth-attentional features for single-image rain removal. In: Proceedings of the IEEE/CVF Conference on Computer Vision and Pattern Recognition. 2019. pp. 8022-8031.
31. Zhang H, Patel VM. Density-aware single image de-raining using a multi-stream dense network. In: Proceedings of the IEEE Conf Comput Vis Pattern Recognit. 2018. pp. 695-704.
32. Li Y, Tan RT, Guo X, Lu J, Brown MS. Rain streak removal using layer priors. In: Proceedings of the IEEE Conf Comput Vis Pattern Recognit. 2016. pp. 2736-2744.